Journal of Geochemical Exploration 159 (2015) 79–92

Contents lists available at ScienceDirect

Journal of Geochemical Exploration

journal homepage: www.elsevier.com/locate/jgeoexp

Assessing the hydrogeochemistry of groundwaters in ophiolite areas of Euboea Island, Greece, using multivariate statistical methods

Nikolaos Voutsis [a], Efstratios Kelepertzis [a], Evangelos Tziritis [b], Akindynos Kelepertsis [a,*]

[a] Faculty of Geology and Geoenvironment, University of Athens, Panepistimiopolis, 157 84, Zographou, Athens, Greece
[b] Hellenic Agricultural Organization "Demeter", Soil and Water Resources Institute, 57400, Sindos Industrial Zone, Greece

ARTICLE INFO

Article history:
Received 19 November 2014
Revised 3 August 2015
Accepted 21 August 2015
Available online 28 August 2015

Keywords:
Hydrogeochemistry
Multivariate analysis
Groundwater
Contamination sources
Euboea Island
Greece

ABSTRACT

Major ion and selected trace element compositions were analyzed in 102 groundwater samples from central and northern areas of Euboea Island, Greece, where both serpentinite dissolution and anthropogenic activities (agricultural) are in action. By integrating hydrogeochemical and two multivariate statistical methods, hierarchical cluster analysis (HCA) and principal component analysis (PCA), the chemistry of these groundwaters was assessed with the aim to understand the evolution of groundwater and assign the major processes that exert control on its composition. HCA classified the groundwater samples into three chemically distinct groups (C1–C3) according to their dominant chemical composition. These three clusters were further categorized by their electrical conductivity values: C1 (median EC: 480 μS/cm), C2 (median EC: 608 μS/cm), C3 (median EC: 1020 μS/cm). PCA was performed to identify the underlying natural and anthropogenic processes affecting the chemistry of these groundwaters. The PCA results can be represented by two principal factors: (1) salinization by seawater intrusion and NO_3^- contamination; and (2) enrichment of groundwater with Mg^{2+}, HCO_3^- and Cr following groundwater–serpentinite interaction. A third trivial component is associated with more local effects of the geological substrate. The three components of the PCA account for 70% of the total variance in the data. Dissolved Cr concentrations (up to 71 μg/L) that rise environmental concerns are more pronounced in the groundwaters from the alluvial coastal area of Politika (C3 water samples). Results of this study demonstrate that appropriate measures should be taken to protect the vital groundwater resources in the alluvial coastal area including the regulation of the amount of chemical fertilizers applied to agricultural soils and the monitoring of groundwater pumping rates.

1. Introduction

Groundwater is an active component of the hydrological cycle that is often recognized as one of the most important resource for drinking and irrigation (Mandel and Shiftan, 1981). Groundwater contamination has become an urgent environmental problem, prompting numerous investigations around the globe to identify chemical patterns in groundwater quality and evaluate potential consequences on environmental compartments and human health. The chemical composition of groundwater is controlled by several natural factors including aquifer lithology, interaction with soils and geological formations of the vadose zone, as well as the relative groundwater flow velocity and the residence time (Appelo and Postma, 2005). In addition, anthropogenic activities such as overexploitation of groundwater resources, agriculture and industry have been typically shown to impact on the groundwater chemistry (examples given by Huang et al., 2013; Jeong, 2001; Kaitantzian et al., 2013; Oren et al., 2004; Spalding and Exner, 1992). Understanding the principal processes that control groundwater quality is not only crucial, in terms of sustainable management of groundwater resources, but also scientifically challenging especially in complex geological and hydrogeological settings. Both hierarchical cluster and principal component analysis have been established as efficient tools in analyzing water-chemistry data and identifying the factors that affect its chemical composition (Cloutier et al., 2008; Güler et al., 2002; Helena et al., 2000; Monjerezi et al., 2011; Singh et al., 2004; Vega et al., 1998).

Ophiolitic rocks occupy around ~1% of the Earth total exposed surface and typically include mafic and ultramafic rocks affected by varying degrees of serpentinization. Groundwaters interacting with ophiolitic rocks are mostly Mg–HCO_3 in composition (Fantoni et al., 2002; Papastamataki, 1977) and are typically characterized by elevated concentrations of Cr and Ni (examples given by Robles-Camacho and Armienta, 2000; Margiotta et al., 2012; Shah et al., 2012) derived from the dissolution of primary and secondary solid phases. Nickel dissolved concentrations are more likely to be low in the case of neutral and alkaline groundwaters, due to its enhanced adsorption onto clays and/or Fe and Mn (hydr)oxides existing in the soil. For that reason the majority of studies have focused on reporting concentrations of naturally occurring Cr in groundwater interacting with ophiolitic rocks in diverse regions

* Corresponding author.
E-mail address: kelepertsis@geol.uoa.gr (A. Kelepertsis).

http://dx.doi.org/10.1016/j.gexplo.2015.08.007
0375-6742/

around the globe (e.g. Fantoni et al., 2002; Gray, 2003; Guertin et al., 2005; Lelli et al., 2014; Mills et al., 2011; Robles-Camacho and Armienta, 2000).

In central Greece, an ongoing number of investigations have outlined the natural elevated background of topsoil with Ni and Cr as result of weathering processes of minerals contained in ultramafic rocks (Kanellopoulos and Argyraki, 2013; Kelepertzis et al., 2013; Lilli et al., 2015; Megremi, 2010; Panagopoulos et al., 2015; Tziritis et al., 2011; Vardaki and Kelepertsis, 1999). In terms of the water chemical composition, the studies have focused either on determining Cr concentrations in groundwater systems (Tziritis et al., 2012; Vasilatos et al., 2008) or on distinguishing the natural from anthropogenic sources of dissolved Cr enrichment (Kelepertzis, 2014; Moraetis et al., 2012; Panagiotakis et al., 2015).

Until now, however, and despite the continuous speculation about the Cr presence even in the drinking water of Greece (Demetriades, 2010; Reimann and Birke, 2010), very little information is known about the regional hydrogeochemistry of groundwaters in areas characterized by extensive ophiolitic occurrences. The lack of systematic hydrogeochemical studies in such areas has led to restricted knowledge of variation in groundwater chemistry when additional factors, such as intense agriculture in coastal areas and excessive application of chemical fertilizers, may affect adversely the water quality. In this article, attention was drawn to investigate the main hydrogeochemical features and processes that affect the chemistry of groundwaters interacting with ophiolitic rocks and their weathered products that participate as fragments in the alluvial aquifers of central and northern areas of Euboea Island, central Greece. The groundwater resources in this region are significant in terms of irrigation and potable water supply. The chemistry of groundwater on the basis of major ions and trace elements is assessed by integrating hydrogeochemical and statistical methods that allowed the different water types and the major natural and anthropogenic processes occurring in the area to be identified, spatially demarcated and described.

2. Description of the study area

Euboea Island is located in central Greece and is characterized by a diverse topographic relief due to the development of plain areas around mountainous regions (Fig. 1). The central part of the Island which is the focal area of this study has a mean altitude of 335 m. The main pattern of land use is represented by forest areas. The majority of the remaining area is devoted to agricultural activities, mineral extraction sites and residential buildings.

According to Katsikatsos et al. (1980) and Katsikatsos et al. (1981), the geological regime of central Euboea (Fig. 2) is characterized by a thick sequence of formations which are consisted at their bottom of a Permian pre-alpine clastic metamorphic substrate. Accordingly follows a series of Triassic–Jurassic dolostones, dolomitic limestones and limestones in intercalations which progressively turn into silicified limestones (these rocks have been simplified to carbonate rocks in Fig. 2); subsequently follows an upper Jurassic tectonometamorphic complex (mélange) of schists and mudstones often containing serpentinized ophiolitic fragments as olistholiths from the overlying parent ophiolitic rocks.

Based on 19 representative ophiolitic rock samples collected from corresponding outcrops in the study area (Voutsis, 2011), the ophiolitic bedrock exhibits high Mg concentrations ranging from 9.6% to 21.9%, low Fe concentrations ranging from 3.8% to 6.0% and very low Al, Ca, Na and K amounts (<1%). With respect to the trace element content, Ni, Cr, Co and Mn are enriched (medians of 2375, 736, 98 and 767 mg kg^{-1} respectively) due to their high natural abundance in ultramafic rocks. Based on mineralogical analysis by X-ray diffraction (Voutsis, 2011), the ophiolitic rocks are dominated by the occurrence of serpentine (antigorite and chrysotile) with lesser olivine (forsterite). In some samples, orthopyroxene (enstatite) and clinopyroxene (diopside) are also present as major mineral phases whereas talc, clinochlore and amphibole (tremolite) occur subordinately. Chromite was not detected by the XRD spectrum, probably because of its low (<5%)

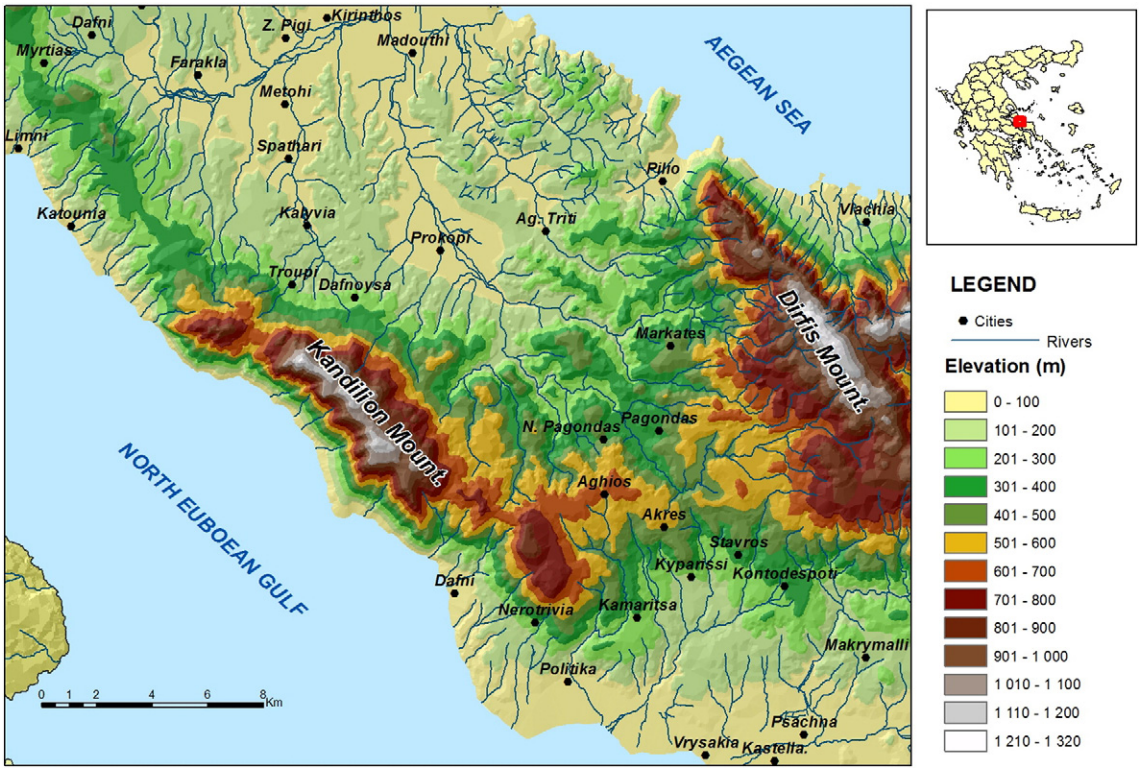

Fig. 1. Topographical map of the study area.

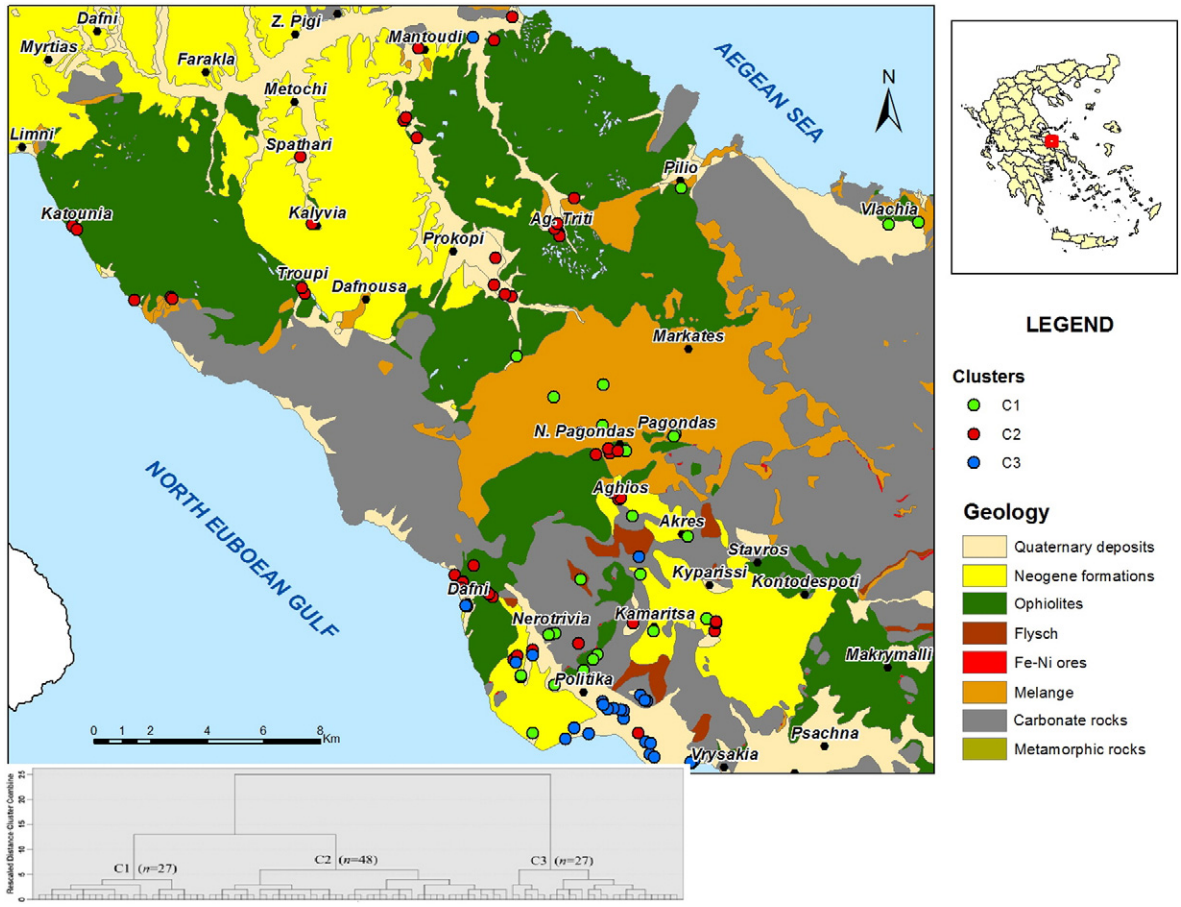

Fig. 2. Simplified geological map of central Euboea (after Katsikatsos et al., 1981) with the results obtained by hierarchical cluster analysis.

contribution. The overall geochemical and mineralogical data for the studied local ophiolites strongly support their characterization as serpentinites (Voutsis, 2011). At the upper members of the ophiolitic formations weathered crusts of rich lateritic horizons are developed, as an eroded, reworked and redeposited ferruginous material, rich in Fe, Ni, Co and Mn (Skarpelis, 2006). Finally the alpine series is completed with a sequence of cretaceous limestones, often highly karstified, and the typical Eocenic flysch. Post-Alpine formations overlie these facies comprising Neogene formations (marls, sandstones etc.) and recent Quaternary alluvial and colluvial fluvio-lacustrine deposits.

Hydrogeological regime is controlled by the development of a number of aquifer systems which are characterized by different permeabilities and productive yields. The most significant aquifers are those developed within the karstified formations at the northeastern and central parts of the study area; the northeastern system (Mantoudi karstic system) consists of confined to semi-confined aquifers (apart from few exceptions where the karstic substrate outcrops) with an overall groundwater flow towards west and southwest (Voutsis, 2011); the central system (Dirfis karstic system) consists of several individual aquifers which are directly recharged by the surrounding mountainous regions without any significant hydraulic connections or lateral crossflows from other systems (Voutsis, 2011). Alluvial aquifers are mainly developed within quaternary deposits and appear low to mediocre yield due to their small spatial extension; in general they are consider as unconfined but depending on their clay content they may turn into partially confined. Another system which is characterized by mediocre yield is the one developed within the fine-grained Neogene formations of southwest (Psachna system) and consists of sandstones, breccias and marly limestones. Finally, variable aquifers of low to mediocre potential are developed within the ophiolitic complex as well as within the mélange due to secondary (tectonic-driven) porosity; aquifer systems in these cases are developed across the highly fractured zones from few to maximum 50–60 meters below surface.

3. Materials and methods

3.1. Sampling and analyses

The water samples were collected in two sampling campaigns during the summer months (dry hydrological period) of 2005 and 2006. A total of 102 groundwater samples (Fig. 2) were selected for the characterization of groundwater chemistry in the study area including boreholes, springs and wells commonly utilized for drinking, domestic and irrigation purposes. Boreholes were pumped prior to sampling for adequate time to flush out the residual water; samples were collected in a 1 L and 50 mL polyethylene bottles for laboratory analyses. The smaller aliquot intended for the determination of metals were filtered on site through 0.45 μm membrane filters and acidified down to pH < 2 with analytical grade HNO_3 (Suprapur 65%). The samples were stored in a portable cooler containing ice packs, transported to the laboratory and refrigerated at 4 °C until analysis. The 1 L polyethylene bottles used for major ion determinations were filtered upon arrival at the laboratory but not acidified.

Parameters such as pH (ISO, 10523-1:1994) and electrical conductivity (EC) (ISO 7888, 1985) were measured in-situ using a temperature compensated multiparameter instrument by WTW® (WTW Multi 350i, Wissenschaftlich-Technische Werkstätten, Germany). Analyses for total concentrations of eight major ions (K^+, Na^+, Ca^{2+}, Mg^{2+}, HCO_3^-, NO_3^-, Cl^-, SO_4^{2-}) and seven trace elements (Cu, Zn, Ni, Cr, Mn, Pb and Cd) were carried out at the Laboratory of Economic Geology and Geochemistry (Faculty of Geology and Geoenvironment, University of Athens)

according to the Standard Methods for the Examination of Water and Wastewater (Clesceri et al., 1989).

Alkalinity (as HCO_3^-) was measured using the titration method [2320-B]. The concentrations of K^+ and Na^+ were determined by flame emission photometry according to the methods [3500-K B] and [3500-Na B], respectively. Nitrate ions were measured by the cadmium reduction method [4500-NO_3 E], SO_4^{2-} by the turbidimetric method [4500-SO_4 E] and Cl^- by the mercuric nitrate method [4500-Cl C] using a Hach DR 4000® spectrophotometer. Calcium ions and Mg^{2+} were determined by flame atomic absorption spectroscopy according to the methods [3500-Ca] and [3500-Mg] using a Perkin Elmer 603® instrument and trace metal elements by graphite furnace atomic absorption spectroscopy (Perkin Elmer 1100B®). Multi-element standard solutions prepared by serial dilution of single certified standards were used for calibration of analytical instruments. Ten random water samples were also analyzed for their major cation and trace element content at the accredited Acme Analytical Laboratories of Canada by ICP-MS with an overall good correlation between the concentrations determined by the two laboratories (R^2 values ranging from 0.90 to 0.99 for all major cations and trace metals).

3.2. Statistical analysis of data

The IBM® SPSS v.22 (2013) software was used to analyze the high dimensional groundwater quality data of the samples. In this study, 11 chemical variables (K^+, Na^+, Ca^{2+}, Mg^{2+}, HCO_3^-, NO_3^-, Cl^-, SO_4^{2-}, Ni, Cr and Zn) were processed using hierarchical cluster analysis (HCA) and principal component analysis (PCA). EC is a parameter with additive characteristics and as a result it was excluded from the multivariate analysis. In this study, concentrations of some chemical parameters (e.g. NO_3^-, Ni, Cr) were lower than the detection limit of the method used for a small number of samples. These values have to be replaced with the aim to become appropriate for the multivariate statistical techniques (Güler et al., 2002). We chose in this research to replace these data by the value of the detection limit (Farnham et al., 2002). HCA has been successfully applied in a number of hydrogeochemical studies to determine if samples can be grouped into distinct hydrochemical groups based on their similarity (Güler et al., 2002; Monjerezi et al., 2011; Yidana, 2010). PCA technique was applied to chemical data to extract the principal factors corresponding to the different natural and anthropogenic processes that exert control on the chemical composition of groundwaters (Cloutier et al., 2008; Güler et al., 2012; Helena et al., 2000; Huang et al., 2013).

Determining the appropriate combination of linkage rule and similarity measurement is one of the key decisions that must be made when performing HCA. Knowing that different techniques can lead to completely different results in HCA (Reimann et al., 2008), we carefully examined all available combinations with the aim to produce the most distinctive groups of groundwaters in terms of their chemical composition. It was found that the Ward's method as a linkage rule followed by the Manhattan distance as similarity measurement resulted in the most favorable outcome, i.e. the samples within each defined cluster were as similar as possible to each other while the differences between the clusters were as large as possible. The results were reported in the form of dendrogram from which the number of clusters was selected. An excellent account of the theory of the various linkage rules and similarity measurements is given by Kaufman and Rousseeuw (1990). Prior to the application of HCA, all the variables were standardized to their corresponding z-scores, as commonly implemented in multivariate HCA ensuring that all chemical parameters are weighed equally (Güler et al., 2002).

PCA is used to reduce the dimensionality of the chemical data set with correlated variables by creating new uncorrelated variables (the PCs) that are linear combination of the original data (Jolliffe, 2002). The varimax rotation method was applied in order to reduce the contribution of variables with minor significance facilitating the interpretation of the output results (Jolliffe, 2002). An important step in PCA is to determine the optimum number of components to retain. In this study, both the Kaiser criterion (Kaiser, 1960) and the scree plot method (Cattell, 1966) were used. The Kaiser criterion eliminates the principal components with eigenvalues smaller than 1. This approach has been criticized in the literature (Costello and Osborne, 2005; Zwick and Velicer, 1986) as it tends to overestimate the number of components. The scree plot is the graphical visualization of the relationship between the eigenvalues and the number of components. In this case, the cut-off is chosen at the point where the function displayed by the scree plot shows an elbow allowing the division of the major components from the trivial components.

4. Results

4.1. Data validation

The chemical analyses were tested for charge balance errors. Calculated charge balance errors were found to be less than or equal to ±10% for the majority of samples, which is an acceptable error for the purposes of the present study (Güler et al., 2002; Kumar et al., 2006; Yaouti et al., 2009). A small percentage (≈20%) appeared to have balance errors over 10%, mainly up to 13%; these water samples were further studied. Charge balance errors favored the cations indicating that a systematic error could be responsible for the observed deviation in electroneutrality. Positive charge balance errors are commonly related to alkalinity measurements (Fritz, 1994). If alkalinity is not measured in the field, it is very likely that precipitation of a carbonate mineral will occur in the sampled bottle. This is particularly true for groundwaters in carbonate terrains that are typically supersaturated with respect to calcite and/or dolomite (Fritz, 1994); as a result, the alkalinity (consisting entirely of bicarbonate in the pH range of the studied waters) will be underestimated.

Variations on the concentrations of dissolved species take on a special importance in multivariate analysis and could potentially end up in different clusters in HCA or factor weights in PCA. Nevertheless, for the present groundwater chemical data set, the removal of the water samples with a charge balance error greater than 10% does not influence the results. The clustering of samples according to the dominant chemical composition and the inclusion of the chemical constituents in the principal components remained the same. We subsequently decided to incorporate all the collected groundwater samples for our discussion providing a more representative groundwater chemical data set for the studied area. Such a treatment does not necessarily weaken the scientific findings revealed by the present study, but it does remind us that hydrogeochemical patterns should be treated by caution, especially for the water samples whose chemistry is influenced by dissolution of carbonate minerals.

4.2. Chemical composition of groundwater

The statistical summary of chemical analyses and field measurements for the 102 groundwater samples are summarized in Table 1. The concentrations of Cd, Mn, Pb and Cu were either very close or below to the detection limit of the analytical technique for most groundwater samples; hence, they have been omitted from further data processing as having negligible impact to hydrogeochemistry. Groundwater was predominantly alkaline (median value 7.8). Electrical conductivity (EC) varied widely from 250 to 3090 μS/cm (median 640 μS/cm). High EC values of some samples are indicative of saline groundwater which is consistent with the presence of high Na^+ and Cl^- concentrations (maximum values of 426 and 627 mg/L respectively). The highest EC values are observed close to coastline suggesting that seawater intrusion may be the mechanism controlling the groundwater chemistry in the alluvial coastal area of Politika (Fig. 3). The concentrations of K^+, Ca^{2+} and Mg^{2+} exhibited low to moderate variation and ranged from 0.3 to 13.1 mg/L, 3.8 to 128 mg/L and 4.4 to 102 mg/L, respectively. On the contrary, high variation was observed for Na^+ with its concentrations ranging

Table 1
Statistical summary of chemical parameters for the groundwater samples ($n = 102$) of the study area.

Parameter	Mean	Minimum	Maximum	Median	Standard deviation
pH	7.79	7.2	8.5	7.8	0.22
EC (μS/cm)	742	250	3090	640	406
K^+ (mg/L)	1.4	0.3	13.1	1	1.8
Na^+ (mg/L)	42.4	3.2	476	27	65.3
Mg^{2+} (mg/L)	42.6	4.4	102	42	26.2
Ca^{2+} (mg/L)	53.1	3.8	128	56	27.5
Cl^- (mg/L)	55	10.2	627	28.5	91.7
HCO_3^- (mg/L)	275	110	439	279.5	68.8
SO_4^{2-}(mg/L)	32.2	2.42	215	16	45.3
NO_3^- (mg/L)	10.6	bdl	82	8.4	15.6
Ni (μg/L)	3.11	bdl	18	2.6	3.34
Cr (μg/L)	10.7	bdl	71	5.2	12.7
Zn (μg/L)	55.5	5	450	9.5	88.5

bdl = below detection limit.

from 3.2 to 476 mg/L (median 27 mg/L). Referring to the major anions, Cl^-, HCO_3^- and SO_4^{2-} showed a great variability in their concentrations ranging from 10.2 to 627 mg/L, 110 to 439 mg/L and 2.42 to 215 mg/L, respectively. Nitrates were present in a moderate range with a maximum concentration of 82 mg/L (median 8.4 mg/L).

Regarding the distribution of Cr in the study area, the median concentration in groundwater was 5.2 μg/L, but as seen on Fig. 4 there are some elevated values (up to 71 μg/L) lying mainly at the alluvial plain areas. Nickel concentrations in general are low (median 2.6 μg/L) and exhibit limited deviation to their values; the higher ones (up to 18 μg/L) are spatially located in areas with ophiolitic occurrences and/or limestones (Fig. 5), which are spatially diverse than those of elevated values for Cr; both of them are supported by geological evidences, either due to Mg-rich mineral dissolution in serpentinites or because of the development of Fe–Ni rich lateritic horizons lying on karstified limestones. Finally, Zn concentrations varied widely from 5 to 450 μg/L with a median value of 9.5 μg/L.

To have a further insight on the probable processes governing groundwater chemistry in respect to major ions, the scatter diagram of Na^+ vs Cl^- has been plotted in meq/L (Fig. 6). It is evident that a considerable number of samples (10%) are clearly affected by seawater intrusion, having Na/Cl ratios lower than 0.78 (Mandel and Shiftan, 1981); the majority of these samples are spatially located close to the coastline at the southwestern part of the coastal Politika basin exhibiting the highest EC values (Fig. 3). However, in the same basin (Politika) there are also few samples with high salinity, shown as outliers in the above Fig. 6. These samples are not related with seawater intrusion as conveyed by their high Na^+/Cl^- ratios and are characterized by elevated Na^+ and NO_3^- values. These observations lead to the conclusion that the salinity source should be attributed chiefly to irrigation water return flow. However, locally increased infiltration conditions may favor aquifer recharge with fresh water ($Ca–HCO_3$ type), which in turn may lead to Na^+ surpluses in the solution due to the reverse ion-exchange process between Ca^{2+} and Na^+ on the surface of clay minerals (Appelo and Postma, 2005).

4.3. Multivariate statistical analyses

The groundwater samples were classified by HCA into three main clusters (C1, C2 and C3) (Fig. 2). Samples with a rescaled distance lower than 6 (Fig. 2) were grouped into the same cluster because this specific evaluation formed chemically distinct clusters in terms of their dominant chemical composition and hydrochemical signature. Differences between the groups are apparent (Table 2). The first cluster includes samples that are characterized by low values of EC (median 444 μS/cm) and low concentrations of Mg^{2+}, Cl^-, HCO_3^-, Cr and Zn in relation to those from C2 and C3. Samples in the second cluster (C2) have EC intermediate between C1 and C3 showing a median value of 608 μS/cm. Similar concentrations of K^+, Na^+ and SO_4^{2-} are observed for C1 and C2 samples, whereas C1 has notably elevated Ca^{2+} concentrations relative to C2 (Fig. 7). Samples in C2 have Mg^{2+} concentrations higher than the ones observed for C1 (Fig. 7). The third cluster (C3)

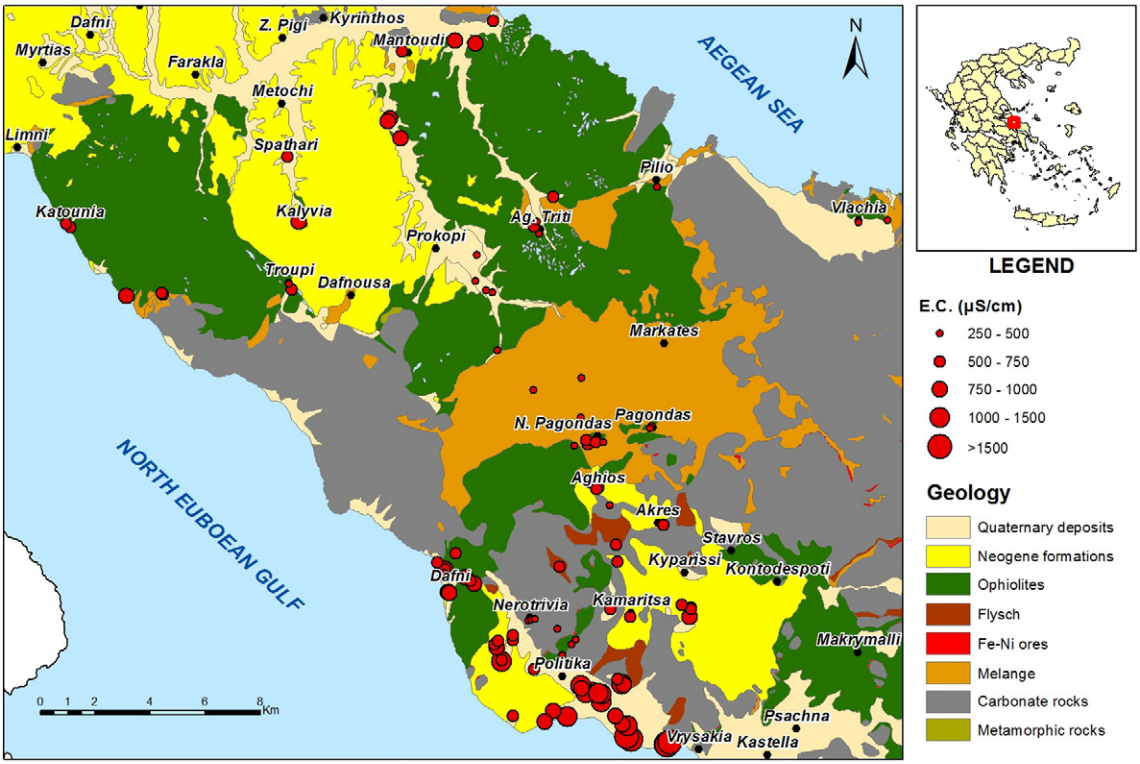

Fig. 3. Spatial distribution of electrical conductivity (EC) values (μS/cm) for the groundwater samples of the study area.

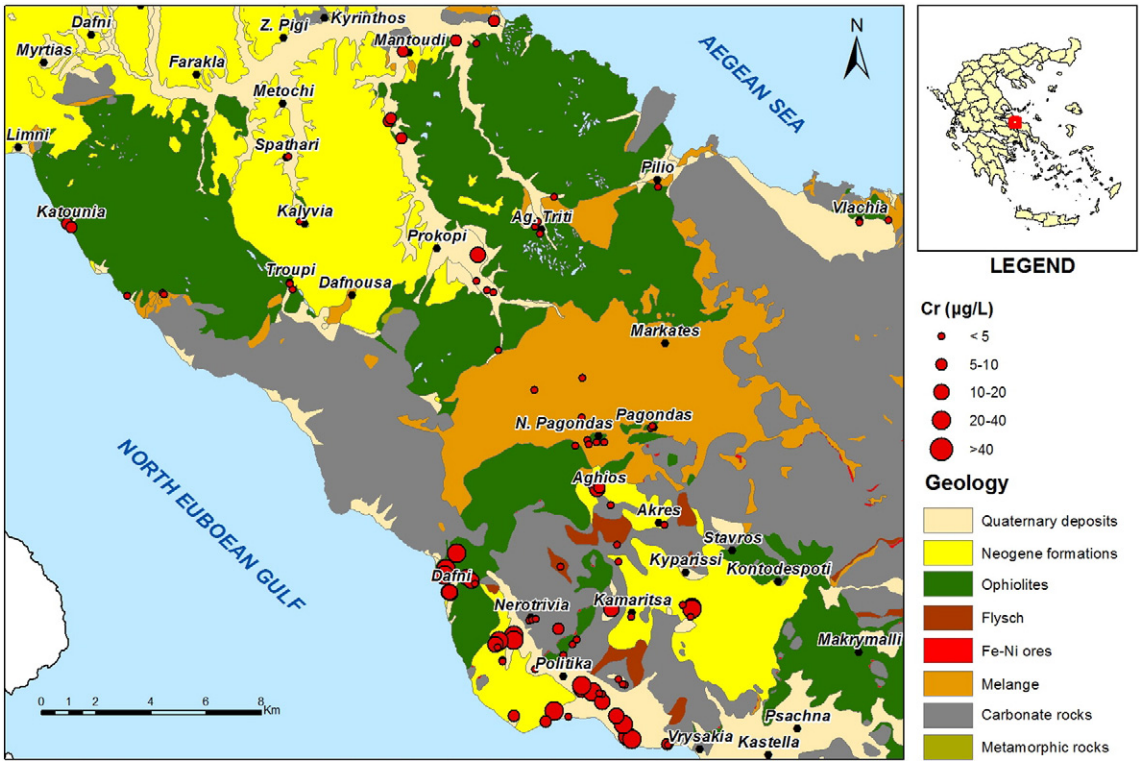

Fig. 4. Spatial distribution of Cr concentrations (μg/L) for the groundwater samples of the study area.

consists of groundwaters exhibiting the highest concentrations of all major ions including NO_3^- (Fig. 7) and an enrichment in their Cr (Fig. 7) and Zn content (medians of 11 and 59 μg/L respectively) compared to the ones in C1 and C2. Nickel levels are similar in all the groundwaters from the three clusters (Fig. 7).

PCA of the groundwater chemical data involved the combination of 11 variables (K^+, Na^+, Ca^{2+}, Mg^{2+}, HCO_3^-, Cl^-, NO_3^-, SO_4^{2-}, Ni, Cr, Zn). The scree plot was used to identify the number of components to be retained; this criterion evolved three PCs having eigenvalues greater than unity and explaining about 70% of the total variance. As shown in

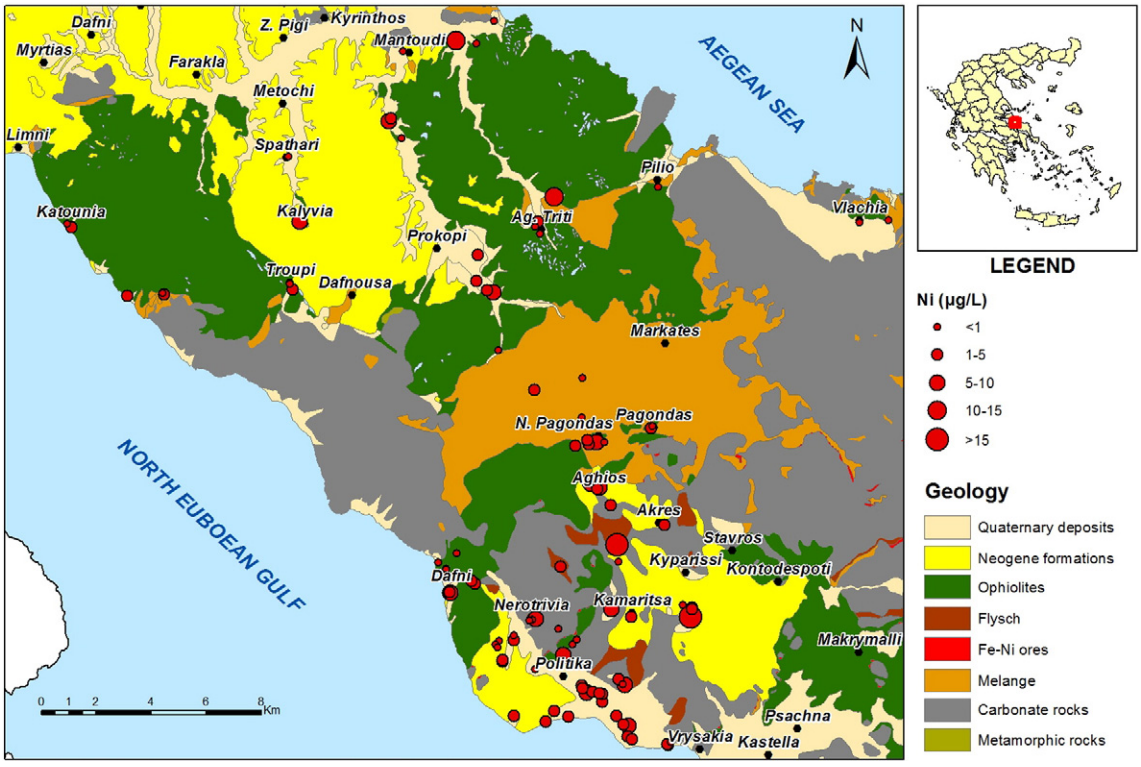

Fig. 5. Spatial distribution of Ni concentrations (μg/L) for the groundwater samples of the study area.

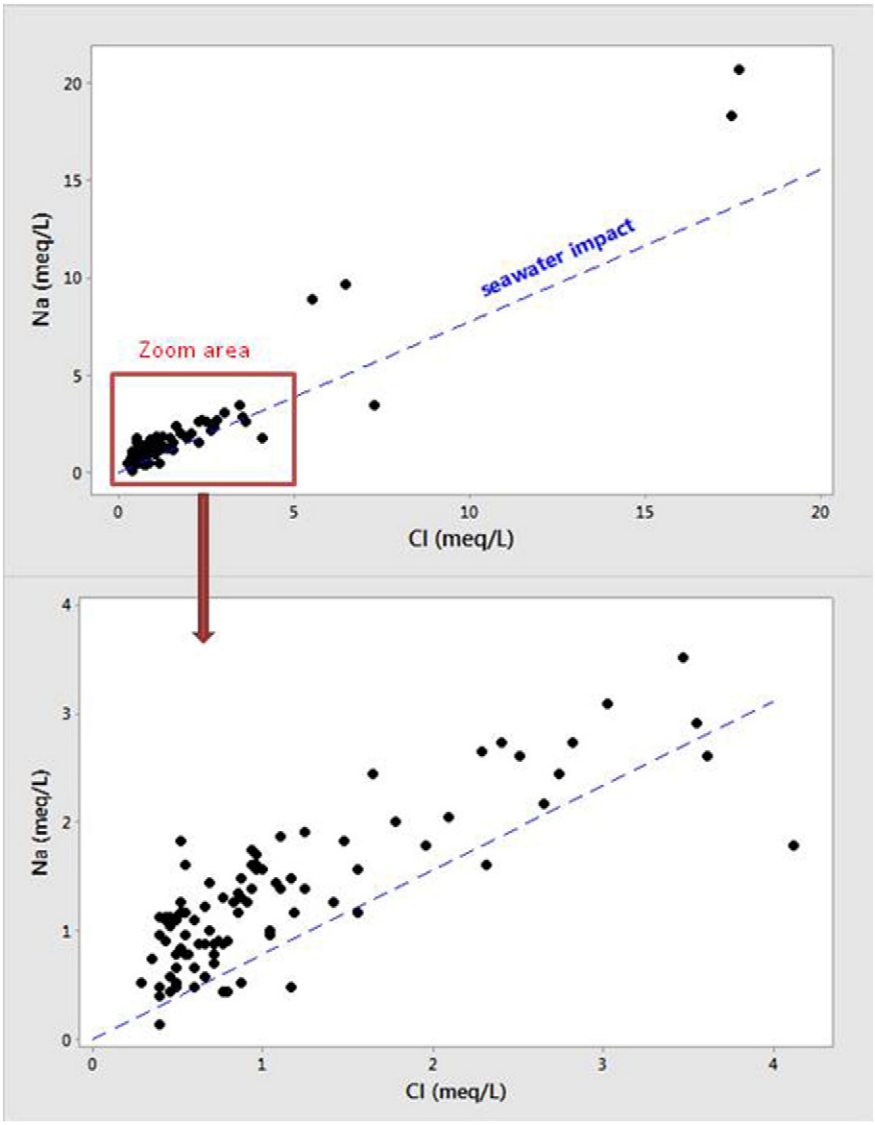

Fig. 6. Bivariate plot showing the relationship between Na^+ and Cl^- (meq/L).

Table 3, the first two components (PC1 and PC2) explain 32.5 and 21.5% of the total variance contained in the original variables. Loadings are in bold for values greater than 0.6. PC1 is associated with the variables K^+, Na^+, SO_4^{2-}, NO_3^- and Cl^- showing loadings between 0.691 and 0.880. PC2 is related to the chemical constituents HCO_3^-, Mg^{2+} and Cr with loadings ranging from 0.690 to 0.935. PC3 is not as important as the first two components and accounts for 15.7% of the variance, indicating that it is more likely to be related with local effects. For this reason, the discussion of PCA (Section 5.2) focuses on results for PC1 and PC2. Component 3 is characterized by medium positive loadings in Ni, Zn and Ca^{2+}. PC3 also incorporates HCO_3^-; however, its contribution is not so clear as evidenced by the loadings of 0.540. Fig. 8 presents the scatter plot of loadings for the three PCs and Fig. 9 depicts the plot of principal component scores for the same components showing the samples labeled with the groundwater clusters.

Table 2
Chemical characteristics of each cluster (median concentrations) produced by hierarchical cluster analysis. Median values of electrical conductivity are also shown.

	C1 ($n = 27$)	C2 ($n = 48$)	C3 ($n = 27$)
EC (μS/cm)	480	608	1020
K^+ (mg/L)	1	0.9	1.7
Na^+ (mg/L)	25	24	60
Ca^{2+} (mg/L)	63	30	74
Mg^{2+} (mg/L)	10	49	55
SO_4^{2-} (mg/L)	12	12	60
Cl^- (mg/L)	17	27	85
HCO_3^- (mg/L)	223	288	311
NO_3^- (mg/L)	3	3	17
Ni (μg/L)	1	2	3
Cr (μg/L)	2	8	11
Zn (μg/L)	7	9	59

5. Discussion

5.1. Hydrogeochemical and hydrodynamical characteristics

The hydrogeochemical and hydrodynamical patterns were assessed with the use of graphical processing through a Piper diagram (Fig. 10). Based on the cationic triangle, it is evident that nearly all cluster samples are plotted within a rectangle area between Ca^{2+} and Mg^{2+} end-members, denoting the impact of the dominant cation as a result of the karstic (Ca-member) and/or the ophiolitic (Mg-member) substrate with the possible contribution of dolostones. Variations between alkalis ($Na^+ + K^+$) within the aforementioned plot area are possibly attributed to ongoing processes like salinization (e.g. seawater intrusion, irrigation water return flow), especially for samples belonging to C3 cluster, or

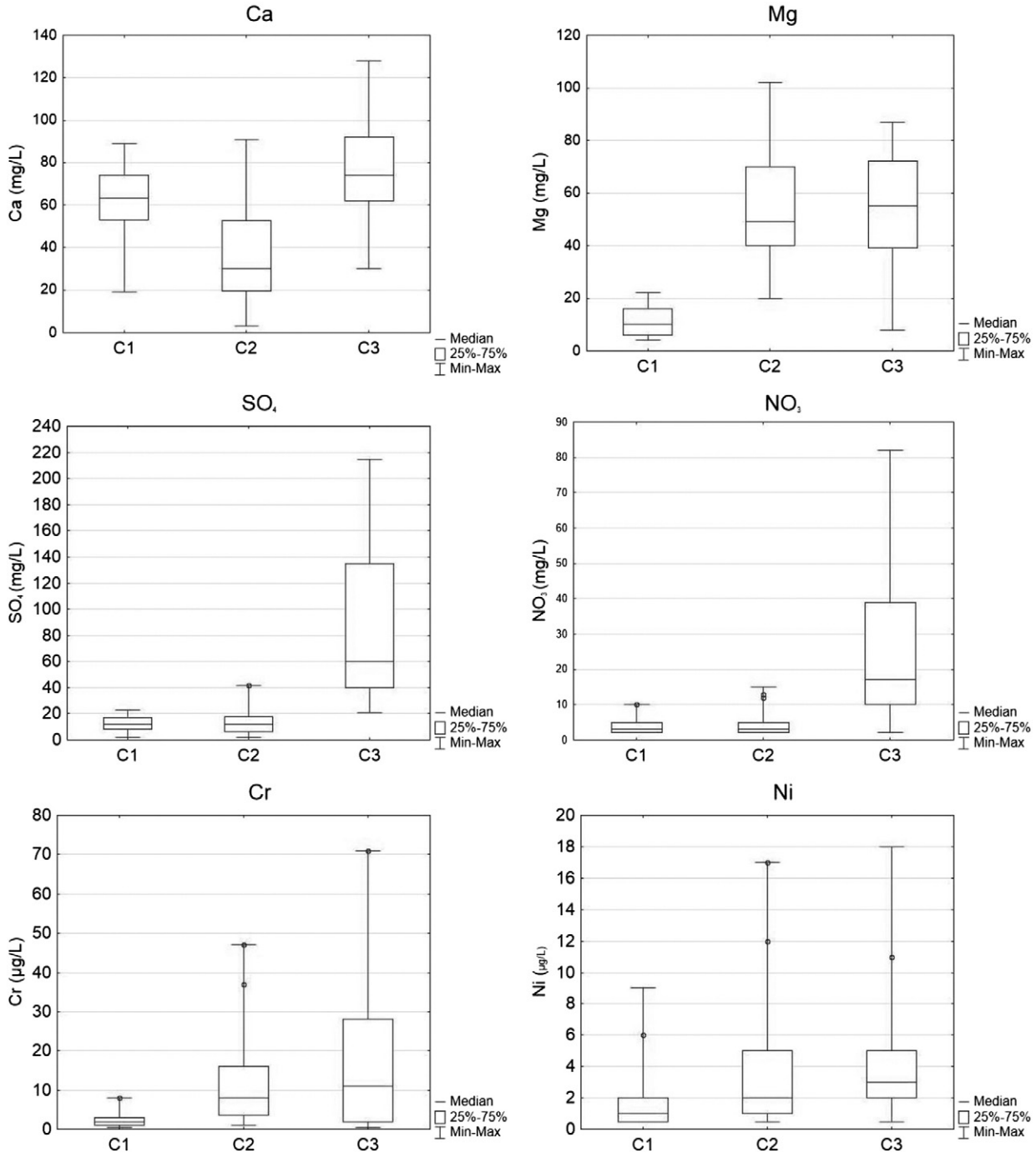

Fig. 7. Box plots of representative major ions and trace elements for groundwater in the three clusters.

diverse hydrodynamical conditions (recharge vs transitional waters). Secondarily, elevated alkali values could be related with the impact of local geology, e.g. the schists contained in tectonic mélange. In respect to the anionic triangle, nearly all samples of clusters C1 and C2 are plotted close to HCO_3 member, as expected, due to the effect from karstic dissolution or olivine weathering (for areas characterized by occurrences of serpentinites). However, samples of C3 are clearly more spread and shifted towards SO_4 and/or Cl members due to the profound salinization effects in accordance with cationic evidences.

Based on Piper diagram we may derive the individual hydrochemical water types of groundwater samples (Table 4) and relate them to the hydrodynamics of the aquifer systems. This approach is based on Frazee (1982) who developed a more specialized interpretive classification scheme for groundwaters using the combined cation and anion graph on Piper diagrams, taking into account not only the dominant ions but also those whose concentrations are significant and are indicative for mix-water types related with hydrodynamical processes (Frazee, 1982; Upchurch, 1992; Harvey et al., 2002).

The dominant hydrochemical type is Mg–Ca–HCO_3 (25 samples) which is representative of recharge (fresh) waters (Frazee, 1982) related with Mg-rich formations; similarly, waters with Mg–HCO_3 type (11 samples) are characterized as recharge waters of the same origin but less affected by Ca^{2+}. Based on Fig. 2, these samples mainly exploit the fissured aquifers of the serpentinites, or are hosted in nearby plain areas that are hydraulically affected by occurrences of serpentinites. Accordingly, the water types of Ca–HCO_3 (9 samples) are indicative of

Table 3
Total variance explained and component loadings for the groundwater samples of the study area (significant loadings are marked in bold).

Variables	Principal components		
	PC1	PC2	PC3
K^+	**0.839**	−0.084	0.008
Na^+	**0.880**	0.138	0.135
Ca^{2+}	0.420	−0.354	**0.620**
Mg^{2+}	0.153	**0.935**	−0.011
SO_4^{2-}	**0.824**	0.168	0.241
HCO_3^-	0.130	**0.690**	0.540
NO_3^-	**0.691**	0.239	0.127
Cl^-	**0.807**	0.379	0.272
Ni	0.023	0.198	**0.692**
Cr	0.199	**0.767**	−0.092
Zn	0.174	−0.073	**0.631**
Explained variance (%)	32.45	21.49	15.71
Cumulative % of variance	32.45	53.97	69.67

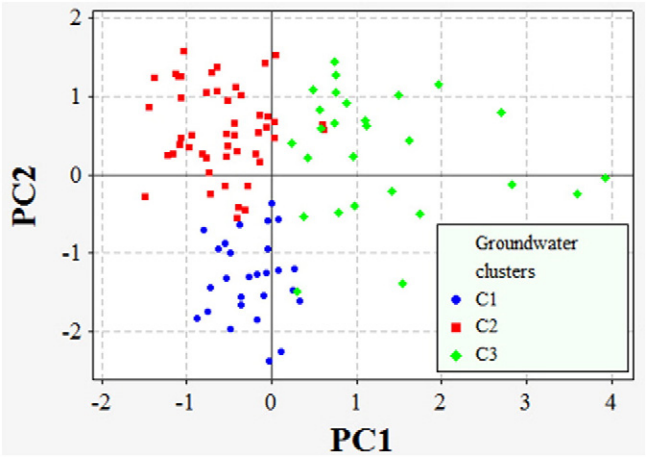

Fig. 9. Plot of principal component scores for the three components showing the water samples labeled with the groundwater clusters.

fresh recharge waters related with karstic areas, as well as those of Ca–Mg–HCO_3 (12) which are related with dolostones. On the contrary, dominant transitional water types include Ca–Na–HCO_3 (12 samples) and Mg–Na–HCO_3 (9). A number of other water types (see Table 4), characterized as transitional and few of them as saline (4 samples), are indicative for the variable processes (e.g. intermixing, salinization, diverse groundwater flow conditions) and the local effect of the geological substrate.

Further to the above assessments, significant patterns are recognized in relation to the three described clusters (C1–C3). Samples of C1 are plotted close to the Ca^{2+} member, reflecting as dominant impact on their hydrogeochemistry the dissolution of the karstic substrate, a fact which is confirmed by the dominant water type of Ca–HCO_3. These samples clearly show fresh recharge waters of direct and fast infiltration conditions; the latter is also deduced for the majority of C1 samples (56%) which are characterized recharge, while transitional (dominant Ca–Na–HCO_3 water type) has a percentage of 44% (Table 4). Sodium's co-dominance in Ca–Na–HCO_3 water type is probably attributed to the effect of mélange formations that include schists with typical Na-bearing minerals (e.g. Na-feldspars); the latter is confirmed by the spatial distribution of these samples as seen in Fig. 2. Alternatively, for those samples located near coastline a possible source of Na^+ enrichment could be the reverse ion-exchange process. Samples with transitional water types hosted in calcareous formations (e.g. limestones) are related

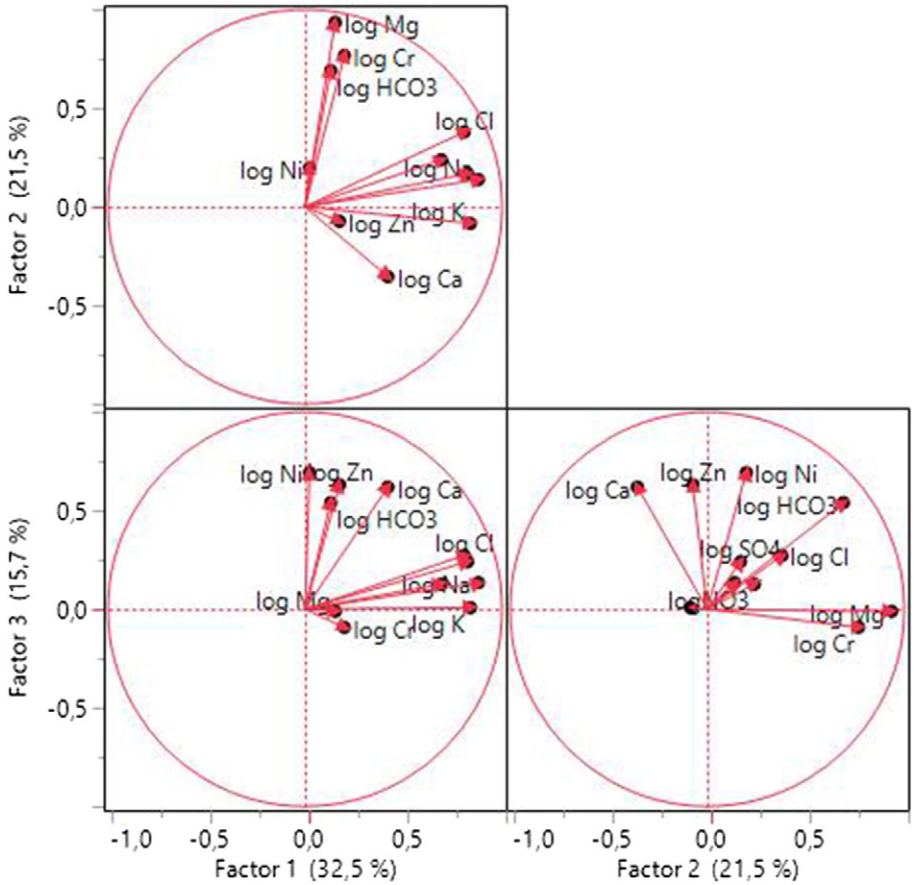

Fig. 8. Scatter plot of loadings for the three identified components of the PCA performed on the groundwater chemical data.

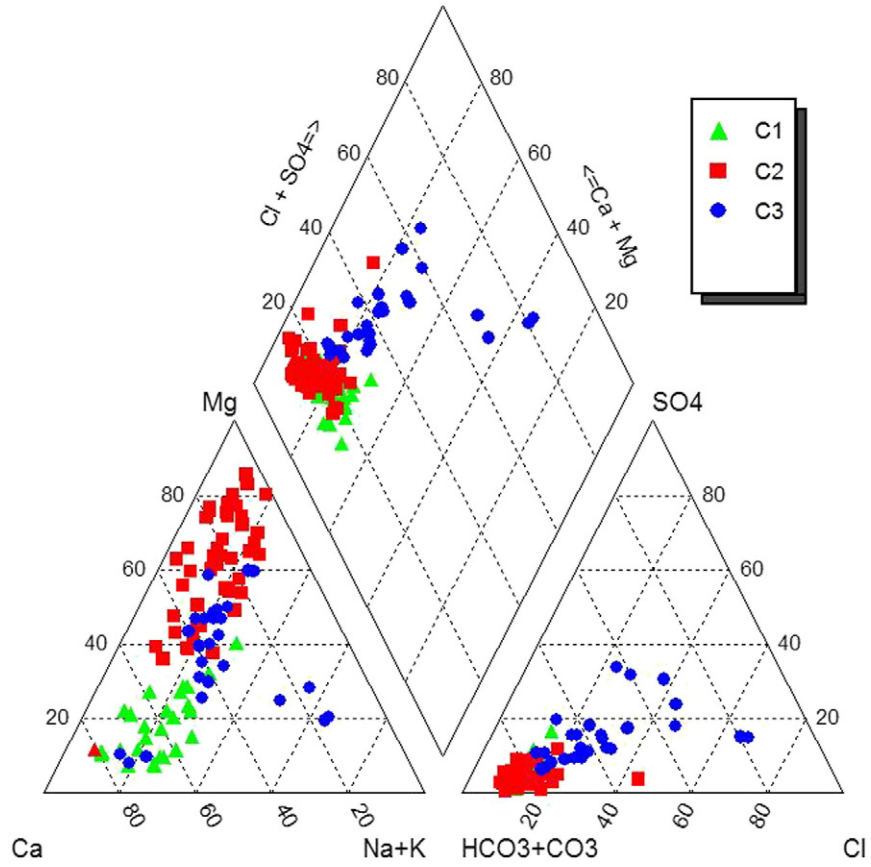

Fig. 10. Piper diagram for the groundwater samples of the study area based on the classification of groundwater samples according to results of HCA.

with deeper aquifers, often affected by overlying aquitards (e.g. mélange) of longer residence times and limit recharge.

Samples belonging to C2 with generally medium EC values (except few of them which are elevated compared to rest) are plotted mainly between the Mg^{2+} member and the hypothetical equiline between Mg^{2+} and Ca^{2+} (50% Ca^{2+} and 50% Mg^{2+}, respectively). These samples are chiefly affected by the serpentinites which either host fissured aquifers of secondary porosity or affect hydrologically connected adjacent alluvial basins; this fact is reflected to the dominant water types of Mg–Ca–HCO_3 and Mg–HCO_3. Even though serpentinites are initially formations of low permeability and yield, subsequent tectonic driven processes favor extensive fracturing and development of alterations, hence creating favorable hydrogeological conditions. As a consequence, the majority of C2 samples are characterized as recharge waters (76%), either related to fissured serpentinites or to shallow sedimentary (alluvial) aquifers consisted of coarse grain material that favors fast and direct infiltration. Samples of this cluster plotted near the Mg^{2+}–Ca^{2+} equiline should be attributed to the impact of dolostones or to transitional-mixed water types.

Finally, samples belonging to C3 cluster with elevated EC values, are clearly more saline and plotted closer to the alkaline member ($Na^{+}+K^{+}$) with nearly balanced concentrations for Mg^{2+} and Ca^{2+} apart from very few exceptions. There is no profound dominant water type (Table 4) and the majority of these samples are characterized as transitional with very limited or negligible recharge; their anionic composition is significantly affected by Cl^{-} and/or SO_4^{2-} as a result of the described salinization processes of seawater intrusion and irrigation water return flow. Their spatial distribution is concentrated in a coastal plain area (Political basin, see Fig. 2) hosted within alluvial deposits.

To have a further insight on the origin of Mg^{2+} which is the dominant cation for most of the groundwater samples, the Mg/Ca ratios in meq/L were used as a definition criterion (Kim et al., 2002; Zhu et al., 2007). Based on Fig. 11 it is clear evident that the rMg^{2+}/Ca^{2+} values which are greater than 0.9 and denote impact from serpentinites are the majority of the samples and are located, as expected, at the northern areas characterized by occurrences of serpentinites and at their adjacent alluvial basins (e.g. eastern of Dafnousa, southern of Mantoudi, and Ag. Triti); the latter is rather important because it implies the hydraulic

Table 4
Groundwater clusters and characterization of hydrochemical water types. In brackets are shown the total number of samples.

Cluster	Hydrochemical water type	Characterization	Percentage
C1	Ca–HCO_3 (7), Ca–Mg–HCO_3 (8)	Recharge waters (15)	56%
	Ca–Na–HCO_3 (11), Mg–Na–HCO_3	Transitional waters (12)	44%
C2	Mg–Ca–HCO_3 (22), Mg–HCO_3 (11), Ca–Mg–HCO_3 (4)	Recharge waters (35)	76%
	Mg–Na–HCO_3 (8), Ca–Mg–HCO_3–Cl, Mg–Ca–HCO_3–Cl, Mg–HCO_3–Cl	Transitional waters (11)	24%
C3	Mg–Ca–HCO_3 (3), Ca–HCO_3 (2)	Recharge waters (5)	18%
	Ca–Mg–HCO_3–Cl (4), Mg–Ca–HCO_3–Cl (5), Mg–Na–HCO_3–Cl (2), Mg–Ca–HCO_3 (2) Mg–Na–HCO_3, Ca–Na–HCO_3, Ca–Na–HCO_3–SO_4, Mg–Ca–Cl–HCO_3, Mg–Ca–HCO_3–SO_4	Transitional waters (19)	68%
	Na–Mg–Cl (2), Na–Ca–Cl–HCO_3, Na–Mg–Cl–HCO_3	Saline waters (4)	14%

connections of these basins, suggesting lateral crossflows and profound impact to their overall hydrogeochemistry as seen previously at the dominant water types. On the contrary, elevated rMg^{2+}/Ca^{2+} values at the southern plain areas (e.g. Politika basin) are more likely attributed to the impact of serpentinized fragments hosted in the alluvial deposits, rather than a direct hydraulic connection with ophiolitic aquifers. The bivariate plot of Mg^{2+} versus Ca^{2+} (in meq/L) indicates that almost all the water samples belonging to the C2 and C3 clusters plot within the serpentinite dissolution domain (Fig. 12).

Values between 0.7 and 0.9 suggest dolomitic origin, but as seen on Fig. 11 these samples are few without any significant spatial distribution. Finally, values below 0.7 which denote impact from calcareous formations are mainly located at the central part of the study area where the karstic substrate mainly occurs (Fig. 11), as well as on the Neogene formations which may locally have significant calcium contribution (e.g. Pliocene limestones). The majority of these water samples belong to cluster C1 from the HCA (Fig. 12). Samples located on mélange formations simply denote the low values of Mg^{2+} compared with Ca^{2+} and are accordingly classified to this category.

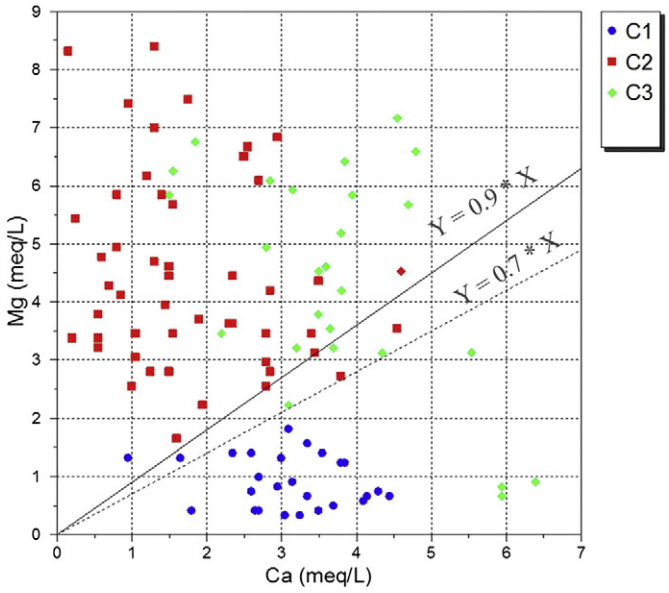

Fig. 12. Bivariate plot showing the relationship between Mg^{2+} and Ca^{2+} (meq/L). Samples are grouped according to their HCA clusters.

5.2. Factors affecting the groundwater chemistry

In groundwater environments characterized by a high degree in chemical data variability, PCA can effectively be applied to highlight the natural and/or anthropogenic factors that control the groundwater chemistry (for example Güler et al., 2012; Huang et al., 2013; Qin et al., 2013). Five chemical parameters in the original data set are contained in PC1. The inclusion of the major solutes Na^+ and Cl^- is indicative of seawater intrusion into the coastal aquifers, as also suggested by the rNa^+/Cl^- (Fig. 6) which evident that 10 samples exhibit values lower than 0.78 (0.33–0.76) which is the critical threshold for the identification of potential seawater intrusion (Mandel and Shiftan, 1981; Richter and Kreitler, 1993). A contribution from ion exchange reactions may also explain some isolated high Na^+ concentrations that are not related to seawater intrusion, as it has already been discussed. In the same area (Politika sub-basin) prevail the groundwaters of cluster C3 (Fig. 2) with high salinity as expressed by the median EC value of 1020 μS/cm. Apart from the obvious seawater effect, the presence of NO_3^- as a major component in PC1 suggests a supplementary contribution to the overall hydrogeochemical status due to intensive agricultural practices and anthropogenic inputs in the coastal agricultural area of Politika. The use of N fertilizers is well established throughout the world and numerous studies have documented systematic increases in NO_3^- concentrations in groundwaters following long-term uncontrolled application of N fertilizers (for example Qin et al., 2013; Zhu et al., 2011). Especially in coastal aquifers where overexploitation triggers salinization effects, the co-existence of sea-water related

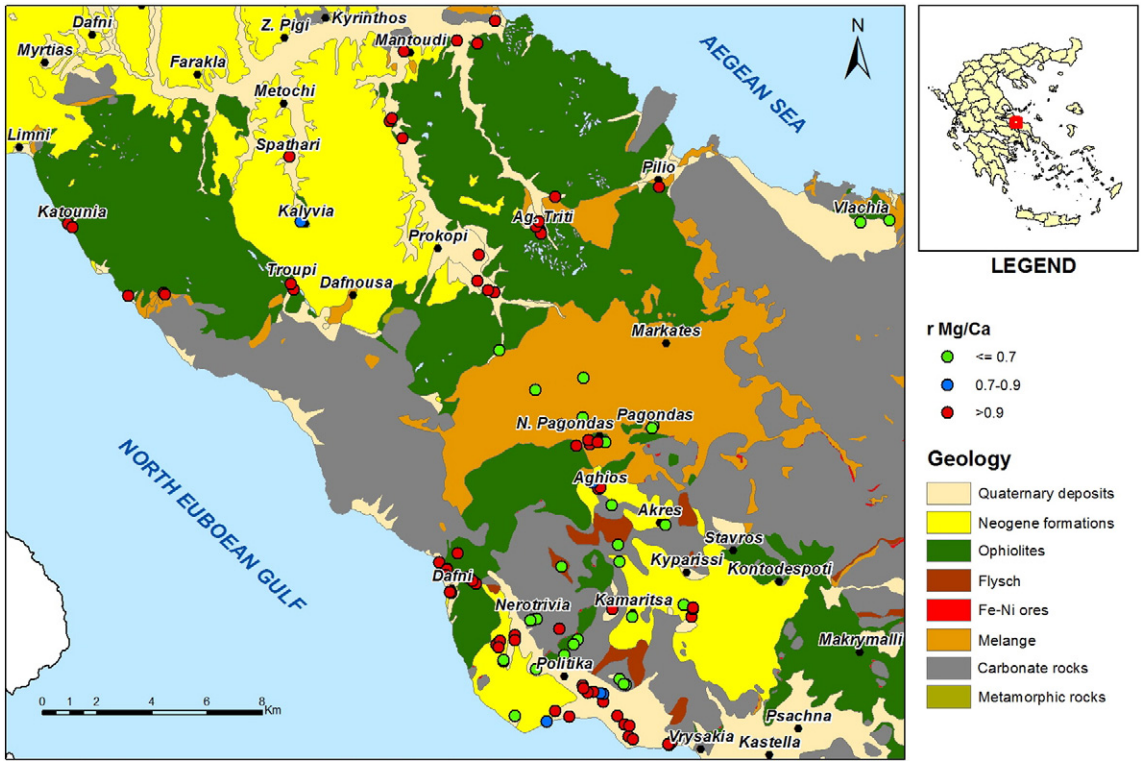

Fig. 11. Map of Mg/Ca ratios for the groundwater samples.

parameters with nitrates is a very common phenomenon (examples are also given by Nakano et al., 2008; Yidana, 2010). The high loadings detected for K^+ and SO_4^{2-} regardless of their typical enrichment in seawater (Böhlke, 2002) may also be associated with other anthropogenic factors, like e.g. irrigation water return flow which increases salinity (García-Garizábal and Causapé, 2010; Barros et al., 2015). In addition, one of the most prominent characteristic of the scatter plot of the principal component scores (Fig. 9) is the clustering of C3 samples in the upper-right and lower-right quadrants of the diagram, associated mainly with increased salinity. Overall, it can be inferred that PC1 is a mixed salinization component representing seawater intrusion and anthropogenic pollution.

PC2 comprises HCO_3^-, Mg^{2+} and Cr and is reflective of water–rock interaction processes referring to the occurrence of serpentinites in the study area. These rocks primarily contain Mg-rich minerals, such as serpentine and olivine (Voutsis, 2011) that are susceptible to chemical weathering though congruent dissolution releasing the ions Mg^{2+} and HCO_3^- (Lelli et al., 2014; Margiotta et al., 2012). The general reaction for olivine, specifically forsterite, dissolution is:

$$Mg_2SiO_4 + 4H_2CO_{3(aq)} \rightarrow 2\,Mg^{2+} + H_4SiO_{4(aq)} + 4HCO_3^-.$$

Moreover, Cr-bearing silicates like olivine, serpentine and pyroxene have been shown to be the primary mineralogical sources of elevated dissolved Cr (Bertolo et al., 2011). Oze et al. (2004) have also reported that chromite grains have the potential to undergo incongruent dissolution and chemical weathering, but the solubility rates are very slow. Although the mineral phases that host Cr have not been identified in the rocks and soils of the investigated area, the solid speciation of Cr in the nearby Thiva basin (central Greece) which exhibits similar geological conditions demonstrated that Cr is mainly bounded with chromite and to a lesser extent with silicates like enstatite and actinolite (Kelepertzis et al., 2013). Samples of C2 occupy the upper-left quadrant of the principal component score plot (Fig. 9) providing evidence that the greatest proportion of the these samples have the groundwater–serpentinite interaction as the principal geochemical process affecting their chemical composition, in agreement with the high rMg^{2+}/Ca^{2+} ratios (Fig. 12). Nevertheless, results of HCA demonstrated that the highest Cr concentrations are contained in the C3 groundwater samples (Fig. 7) that exhibit the highest salinity values and are located in the alluvial coastal area of Politika (median Cr concentration of 11 μg/L). Indeed, higher values of Cr are expected to occur in aquifers of alluvial sediments that contain weathered ultramafic fragments derived from the surrounding serpentinites (Mills et al., 2011). On the opposite, C1 and C2 water samples located further inland (Fig. 2) show in general lower Cr concentrations (medians of 2 and 8 μg/L respectively). This can be ascribed to the low contact time and surface area of the Cr-bearing minerals of the geological substrate in the case of groundwater interacting with serpentinites, as opposed to the weathered serpentinized fragments of the alluvial basins that may undergo a more rapid dissolution (Kaprara et al., 2015). It is noticed, however, that a clear difference in the Cr content is observed for C2 samples compared to C1. In particular, Cr concentrations range from 1 μg/L to 47 μg/L for C2 samples, with 17 out of 48 samples exhibiting concentrations higher than 10 μg/L. On the opposite, the majority of C1 samples are characterized by low Cr content (maximum 8 μg/L). This deviation between C1 and C2 clusters is attributed to the different impact of the geology; as noted from Fig. 2, samples with lower Cr content (C1) are affected by the ophiolitic fragments of tectonic mélange while samples of C2 by ophiolitic rock masses involving the widespread occurrence of serpentinites, as it has already been mentioned.

Interestingly, Ni was dissociated from PC2, despite its participation in the crystal structure of olivine and serpentine (Kelepertzis et al., 2013). Elevated dissolved Ni concentrations deriving from the dissolution of Ni-bearing silicates are generally anticipated under morphological and geochemical conditions that do not support the formation of secondary mineral phases able to absorb mobile ions like Ni^{2+} (Giammetta et al., 2004). Such conditions may exist in areas with higher elevations that do not favor the formation of an extensive weathering soil cover (see Figs. 1 and 5). Secondary minerals typically include clays and Fe–Mn hydr(oxides) and their accumulation in soil environments provide a significant host for Ni sequestration (Oze et al., 2004). To strengthen this interpretation, it is noted that the groundwaters ($n = 40$) in the nearby Thiva basin have very low (<2 μg/L) Ni concentrations (Korres and Perivolaris, 2011) as a result of the occurrence of smectites, goethite and Mn oxides that have trapped the released Ni (Kelepertzis et al., 2013); nevertheless, they contain significant Cr dissolved concentrations reaching a maximum of 212 μg/L (Tziritis et al., 2012).

Finally, the trivial component (PC3) involves Ni and Ca and is a representation of the influence of the existing lateritic Fe–Ni deposits on the groundwater chemistry. According to the geological map of the area (Katsikatsos et al., 1981) there are many outcrops of Fe-Ni ore deposits related to serpentinized ultramafic rocks. These deposits are resting as mechanically reworked laterite detritus on karstified Triassic–Jurassic carbonates (Valeton et al., 1987). The incorporation of HCO_3^- in PC3 with medium loadings provides further evidence for the carbonate dissolution according to the reaction:

$$CaCO_{3(s)} + H^+_{(aq)} \rightarrow Ca^{2+}{}_{(aq)} + HCO_3{}^-{}_{(aq)}.$$

The inclusion of Zn in this component is possibly linked to the groundwater interaction with rock fragments of ophiolitic origin, especially from their upper horizons of pillow lavas that may be enriched with this metal (Bortolotti et al., 2008; Saccani et al., 2008). We interpret PC3 as a geogenic component related to local effects of natural weathering processes of the geological substrate.

6. Conclusions

The hydrogeochemical characteristics and the processes affecting the chemistry of groundwaters interacting with serpentinites have been evaluated in central and northern areas of Euboea Island, Greece, on the basis of major ion and selected trace element composition. The results demonstrate that the groundwater is alkaline in nature, with Mg^{2+} and HCO_3^- as the dominant cation and anion, respectively. The multivariate statistical methods (HCA and PCA) were particularly effective in this groundwater data set for characterizing the water chemistry because of the highly variable chemical composition influenced by both natural and anthropogenic processes. The HCA classified the 102 groundwater samples in 3 distinct clusters (C1–C3) with a dominant hydrochemical type of Mg–(Ca)–HCO_3. These clusters were further categorized by their electrical conductivity values: C1 (median EC: 480 μS/cm), C2 (median EC: 608 μS/cm), and C3 (median EC: 1020 μS/cm). PCA results have shown that two principal processes are responsible for the creation of these water types: (1) salinization by seawater intrusion and NO_3^- contamination; and (2) water–serpentinite interaction resulting to the enrichment of groundwater with Mg^{2+}, HCO_3^- and Cr. The dissociation of Ni from the second component is attributed to the absence of secondary minerals able to trap the released Ni in areas with higher elevations and to the individual influence of the Fe–Ni ore deposits on the groundwater chemistry, as revealed in the trivial component PC3. A salient feature of the investigated groundwaters is the enrichment in the dissolved Cr concentrations occurring in the Politika alluvial coastal area (C3 groundwater samples with high conductivity values) occupied by the products from the weathering and erosion of the serpentinites. The specific mechanisms for the enhanced Cr mobilization in the alluvial aquifers certainly need further clarification, especially considering the possible contribution of agricultural activities to the generation rates of Cr (Mills et al., 2011), but results of this study do increase our knowledge for the groundwater chemical composition in areas where both serpentinite dissolution and anthropogenic processes are in action.

Acknowledgments

We would like to thank Dr Ioannis Mitsis and Dr Dimitris Alexakis for their assistance in chemical analyses at the Laboratory of Economic Geology and Geochemistry, Faculty of Geology and Geoenvironment, University of Athens. We thank the anonymous reviewers of the Journal for their suggestions that improved the scientific soundness of this manuscript.

References

Appelo, C.A.J., Postma, D., 2005. Geochemistry, Groundwater and Pollution. Second edition. A.A. Balkema, Rotterdam.

Barros, R., Isidoro, D., Aragüés, R., 2015. Three study decades on irrigation performance and salt concentrations and loads in the irrigation return flows of La Violada irrigation district (Spain). Agric. Ecosyst. Environ. 151, 44–52.

Bertolo, R., Bourotte, C., Marcolan, L., Oliveira, S., Hirata, R., 2011. Anomalous content of chromium in a Cretaceous sandstone aquifer of the Bauru Basin, state of São Paulo, Brazil. J. S. Am. Earth Sci. 31, 69–80.

Böhlke, J.-K., 2002. Groundwater recharge and agricultural contamination. Hydrogeol. J. 10, 153–179.

Bortolotti, V., Chiari, M., Marcucci, M., Photiades, A., Principi, G., Saccani, E., 2008. New geochemical and age data on the ophiolites from the Othrys area (Greece). Implication for the Triassic evolution of the Vardar Ocean. Ofioliti 33, 135–151.

Cattell, R.B., 1966. The scree test for the number of factors. Multivar. Behav. Res. 1, 245–276.

Clesceri, L., Greenberg, A., Eaton, A., 1989. Standard Methods for the Examination of Water and Wastewater. 20th edition. APHA-AWWA-WEF, Washington, DC.

Cloutier, V., Lefebvre, R., Therrien, R., Savard, M.M., 2008. Multivariate statistical analysis of geochemical data as indicative of the hydrogeochemical evolution of groundwater in a sedimentary rock aquifer system. J. Hydrol. 353, 294–313.

Costello, A.B., Osborne, J.W., 2005. Best practices in exploratory factor analysis: four recommendations for getting the most from your analysis. Pract. Assess. Res. Eval. 10, 1–9.

Demetriades, A., 2010. General ground water geochemistry of Hellas using bottled water samples. J. Geochem. Explor. 107, 283–298.

Fantoni, D., Brozzo, G., Canepa, M., Cipolli, F., Marini, L., Ottonello, G., Zuccolini, M.V., 2002. Natural hexavalent chromium in groundwaters interacting with ophiolitic rocks. Environ. Geol. 42, 871–882.

Farnham, I.M., Singh, A.K., Stetzenbach, K.J., Johannesson, K.H., 2002. Treatment of nondetects in multivariate analysis of groundwater geochemistry data. Chemom. Intell. Lab. Syst. 60, 265–281.

Frazee, J.M., 1982. Geochemical pattern analysis: method of describing the southeastern limestone regional aquifer system. In: Beck, B.F. (Ed.), Studies of the hydrogeology of the southeastern United StatesAmericus, Special Publications: No. 1. Georgia Southwestern College, pp. 46–58.

Fritz, S.J., 1994. A survey of charge–balance errors on published analyses of potable ground and surface waters. Ground Water 32, 539–546.

García-Garizábal, I., Causapé, J., 2010. Influence of irrigation water management on the quantity and quality of irrigation return flows. J. Hydrol. 385, 36–43.

Giammetta, R., Telesca, A., Mongelli, G., 2004. Serpentinites–water interaction in the S. Severino area, Lucanian Apennines, southern Italy. GeoActa 3, 25–33.

Gray, D.J., 2003. Naturally occurring Cr6 + in shallow groundwaters of the Yilgarn Craton, Western Australia. Geochem. Explor. Environ. Anal. 3, 359–368.

Guertin, J., Jacobs, J., Avakian, C. (Eds.), 2005. Chromium (VI) Handbook. Written by Independent Environmental Technical Evaluation Group (IETEG). CRC Press.

Güler, C., Thyne, G.D., McCray, J.E., Turner, A.K., 2002. Evaluation of graphical and multivariate statistical methods for classification of water chemistry data. Hydrogeol. J. 10, 455–474.

Güler, C., Kurt, M.A., Alpaslan, M., Akbulut, C., 2012. Assessment of the impact of anthropogenic activities on the groundwater hydrology and chemistry in Tarsus coastal plain (Mersin, SE Turkey) using fuzzy clustering, multivariate statistics and GIS techniques. J. Hydrol. 414–415, 435–451.

Harvey, W., Krupa, S., Gefvert, C., Mooney, R., Choi, J., King, S., Giddings, J., 2002. Interactions between surface water and groundwater and effects on mercury transport in the north–central Everglades. U.S. Department of the Interior, U.S. Geological Survey, Water Resources Investigations Report 02–450p. 82.

Helena, B., Pardo, R., Vega, M., Barrado, E., Fernández, J.M., Fernández, L., 2000. Temporal evolution of groundwater composition in an alluvial aquifer (Pisuerga river, Spain) by principal component analysis. Water Res. 34, 807–816.

Huang, G., Sun, J., Zhang, Y., Chen, Z., Liu, F., 2013. Impact of anthropogenic and natural processes on the evolution of groundwater chemistry in a rapidly urbanized coastal area, South China. Sci. Total Environ. 463–464, 209–221.

IBM Corp. Released, 2013. IBM SPSS Statistics for Windows, Version 22.0. IBM Corp., Armonk, NY.

ISO (International Standards Organisation), 1985. Water Quality — Determination of Electrical Conductivity. ISO, p. 7888.

ISO (International Standards Organisation), 1994. Water Quality — Determination of pH. ISO 1–10523.

Jeong, C.H., 2001. Effect of land use and urbanization on hydrochemistry and contamination of groundwater from Taejon area, Korea. J. Hydrol. 253, 194–210.

Jolliffe, I.T., 2002. Principal Component Analysis. 2nd edition. Springer-Verlag, New York.

Kaiser, H.F., 1960. The application of electronic computers to factor analysis. Educ. Psychol. Meas. 20, 141–151.

Kaitantzian, A., Kelepertzis, E., Kelepertsis, A., 2013. Evaluation of the sources of contamination in the suburban area of Koropi-Markopoulo, Athens, Greece. Bull. Environ. Contam. Toxicol. 91, 23–28.

Kanellopoulos, C., Argyraki, A., 2013. Soil baseline geochemistry and plant response in areas of complex geology. Application to NW Euboea, Greece. Chem. Erde-Geochem. 73, 519–532.

Kaprara, E., Kazakis, N., Simeonidis, K., Coles, S., Zouboulis, A.I., Samaras, P., Mitrakas, M., 2015. Occurrence of Cr(VI) in drinking water of Greece and relation to the geological background. J. Hazard. Mater. 281, 2–11.

Katsikatsos, G., Fytrolakis, N., Perdikatsis, V., 1980. Contribution to the genesis of lateritic deposits of the upper Cretaceous transgression in Attica and central Euboea (Greece). Proceedings of International Symposium in Metallogeny of Mafic and Ultramafic Complexes. The Eastern Mediterranean–Western Asia Area and its Comparison With Similar metallogenic Environments in the World, Athens, pp. 257–265.

Katsikatsos, G., Koukis, G., Fytikas, M., Anastopoulos, J., Kanaris, J., (1981). Geological Map of Greece, Scale 1:50.000, Psachna-Pilion Sheet. Greek Institute of Geology And Mineral Exploration.

Kaufman, L., Rousseeuw, P.J., 1990. Finding Groups in Data: An Introduction to Cluster Analysis. John Wiley and Sons Inc., NY.

Kelepertzis, E., 2014. Investigating the sources and potential health risks of environmental contaminants in the soils and drinking waters from the rural clusters in Thiva area (Greece). Ecotoxicol. Environ. Saf. 100, 258–265.

Kelepertzis, E., Galanos, E., Mitsis, I., 2013. Origin, mineral speciation and geochemical baseline mapping of Ni and Cr in agricultural topsoils of Thiva valley (central Greece). J. Geochem. Explor. 125, 56–68.

Kim, J., Kim, R., Lee, J., Chang, H., 2002. Hydrogeochemical characterization of major factors affecting the quality of shallow groundwater in the coastal area at Kimje in South Korea. Environ. Geol. 44, 189–478.

Korres, G., Perivolaris, D., 2011. Environmental and Geochemical Study of Groundwaters in the Wider Area of Thiva, Southern of Yliki Lake Dissertation thesis Department of Geology and Geoenvironment, University of Athens.

Kumar, M., Ramanathan, Al, Rao, M.S., Kumar, B., 2006. Identification and evaluation of hydrogeochemical processes in the groundwater environment of Delhi, India. Environ. Geol. 50, 1025–1039.

Lelli, M., Grassi, S., Amadori, M., Franceschini, F., 2014. Natural Cr(VI) contamination of groundwater in the Cecina coastal area and its inner sectors (Tuscany, Italy). Environ. Earth Sci. 71, 3907–3919.

Lilli, M.A., Moraetis, D., Nikolaidis, N.P., Karatzas, G.P., Kalogerakis, N., 2015. Characterization and mobility of geogenic chromium in soils and river bed sediments of Asopos basin. J. Hazard. Mater. 281, 12–19.

Mandel, S., Shiftan, Z.L., 1981. Groundwater Resources: Investigation and Development. Academic Press, New York (269 pp.).

Margiotta, S., Mongelli, G., Summa, V., Paternoster, M., Fiore, S., 2012. Trace element distribution and Cr(VI) speciation in Ca–HCO_3 and Mg–HCO_3 spring waters from the northern sector of the Pollino massif, southern Italy. J. Geochem. Explor. 115, 1–12.

Megremi, I., 2010. Distribution and bioavailability of Cr in central Euboea, Greece. Cen. Eur. J. Geosci. 2, 103–123.

Mills, C.T., Morrison, J.M., Goldhaber, M.B., Ellefsen, K.J., 2011. Chromium(VI) generation in vadose zone soils and alluvial sediments of the southwestern Sacramento Valley, California: a potential source of geogenic Cr(VI) to groundwater. Appl. Geochem. 26, 1488–1501.

Monjerezi, M., Vogt, R.D., Aagaard, P., Saka, J.D.K., 2011. Hydro-geochemical processes in an area with saline groundwater in lower Shire River valley, Malawi: an integrated application of hierarchical cluster and principal component analysis. Appl. Geochem. 26, 1399–1413.

Moraetis, D., Nikolaidis, N.P., Karatzas, G.P., Dokou, Z., Kalogerakis, N., Winkel, L.H.E., Palaiogianni-Bellou, A., 2012. Origin and mobility of hexavalent chromium in North-Eastern Attica, Greece. Appl. Geochem. 27, 1170–1178.

Nakano, T., Tayasu, I., Yamada, Y., Hosono, T., Igeta, A., Hyodo, F., Ando, A., Saitoh, Y., Tanaka, T., Wada, E., Yachi, S., 2008. Effect of agriculture on groundwater quality of Lake Biwa tributaries, Japan. Sci. Total Environ. 389, 132–148.

Oren, O., Yechieli, Y., Böhlke, J.K., Dody, A., 2004. Contamination of groundwater under cultivated fields in an arid environment, central Arava Valley, Israel. J. Hydrol. 290, 312–328.

Oze, C., Fendorf, S., Bird, D., Coleman, R.G., 2004. Chromium geochemistry in serpentinized ultramafic rocks and serpentine soils from the Franciscan Complex of California. Am. J. Sci. 304, 67–101.

Panagiotakis, I., Dermatas, D., Vatseris, C., Chrysochoou, M., Papassiopi, N., Xenidis, A., Vaxevanidou, K., 2015. Forensic investigation of a chromium(VI) groundwater plume in Thiva, Greece. J. Hazard. Mater. 281, 27–34.

Panagopoulos, I., Karayannis, A., Kollias, K., Xenidis, A., Papasioppi, N., 2015. Investigation of potential soil contamination with Cr and Ni in four metal finishing facilities at Asopos industrial area. J. Hazard. Mater. 281, 2–26.

Papastamataki, A., 1977. The alkalinity and the chemical composition of springs issuing from peridotites. Ann. Géol. Pays Hellén. 28, 551–556.

Qin, R., Wu, Y., Xu, Z., Xie, D., Zhang, C., 2013. Assessing the impact of natural and anthropogenic activities on groundwater quality in coastal alluvial aquifers of the lower Liaohe River Plain, NE China. Appl. Geochem. 31, 142–158.

Reimann, C., Birke, M. (Eds.), 2010. Geochemistry of European Bottled Waters. Borntraeger Science Publishers, Stuttgart, Germany.

Reimann, C., Filzmoser, P., Garrett, R., Dutter, R., 2008. Statistical Data Analysis Explained: Applied Environmental Statistics with R. Wiley-Blackwell, Chichester.

Richter, C., Kreitler, C., 1993. Geochemical Techniques for Identifying Sources of Ground-Water Salinization. CRC Press.

Robles-Camacho, J., Armienta, M.A., 2000. Natural chromium contamination of groundwater at León Valley, México. J. Geochem. Explor. 68, 167–181.
Saccani, E., Photiades, A., Santato, A., Zeda, O., 2008. New evidence for supra-subduction zone ophiolites in the Vardar zone of Northern Greece. Implications for the tectono-magmatic evolution of the vardaroceanic basin. Ofioliti 33, 65–85.
Shah, M.T., Ara, J., Muhammad, S., Khan, S., Tariq, S., 2012. Health risk assessment via surface water and sub-surface water consumption in the mafic and ultramafic terrain, Mohmand agency, northern Pakistan. J. Geochem. Explor. 118, 6–67.
Singh, K.P., Malik, A., Mohan, D., Sinha, S., 2004. Multivariate statistical techniques for the evolution of spatial and temporal variations in water quality of Gomti River (India) — a case study. Water Res. 38, 3980–3992.
Skarpelis, N., 2006. Lateritization processes of ultramafic rocks in Cretaceous times: the fossil weathering crusts of mainland Greece. J. Geochem. Explor. 88, 325–328.
Spalding, R.F., Exner, M.E., 1992. Occurrence of nitrate in groundwater — a review. J. Environ. Qual. 22, 392–402.
Tziritis, E., Kelepertsis, A., Fakinou, G., 2011. Geochemical status and interactions between soil and groundwater systems in the area of Akrefnio, Central Greece. Risk assessment under the scope of mankind and natural environment. J. Water Land Dev. 127–144.
Tziritis, E., Kelepertzis, E., Korres, G., Perivolaris, D., Repani, S., 2012. Hexavalent chromium contamination in groundwaters of Thiva basin, central Greece. Bull. Environ. Contam. Toxicol. 89, 1073–1077.
Upchurch, S.B., 1992. Quality of water in Florida's aquifer systems. In: Maddox, G.L., et al. (Eds.), Florida's Ground Water Quality Monitoring Program: Background Hydrogeochemistry. Florida Geological Survey, Talahassee, Fla (364 pp.).
Valeton, I., Biermann, M., Reche, R., Rosenberg, F., 1987. Genesis of nickel laterites and bauxites in Greece during the Jurassic and Cretaceous, and their relation to ultrabasic parent rocks. Ore Geol. Rev. 2, 359–404.
Vardaki, C., Kelepertsis, A., 1999. Environmental impact of heavy metals (Fe, Ni, Cr, Co) in soils waters and plants of Triada in Euboea from ultrabasic rocks and nickeliferous mineralization. Environ. Geochem. Health 21, 211–226.
Vasilatos, C., Megremi, I., Economou, M., Mitsis, I., 2008. Hexavalent chromium and other toxic elements in natural waters in the Thiva–Tanagra–Malakasa Basin, Greece. Hell. J. Geosci. 43, 57–66.
Vega, M., Pardo, R., Barrado, E., Deban, L., 1998. Assessment of seasonal and polluting effects on the quality of river water by exploratory data analysis. Water Res. 32, 3581–3592.
Voutsis, N., 2011. Weathering rates of ultrabasic rocks in Euboea Island and controls of the chemical composition of groundwaters and surface waters PhD Thesis National and Kapodistrian University of Athens, Faculty of Geology and Geoenvironment.
Yaouti, F.E., Mandour, A.E., Khattach, D., Benavente, J., Kaufmann, O., 2009. Salinization processes in the unconfined aquifer of Bou-Areg (NE Morocco): a geostatistical, geochemical, and tomographic study. Appl. Geochem. 24, 16–31.
Yidana, S.M., 2010. Groundwater classification using multivariate statistical methods: Southern Ghana. J. Afr. Earth Sci. 57, 455–469.
Zhu, G.F., Li, Z.Z., Su, Y.H., Ma, J.Z., Zhang, Y.Y., 2007. Hydrogeochemical and isotope evidence of groundwater and recharge in Minqin Basin, Northwest China. J. Hydrol. 333, 239–251.
Zhu, B., Yang, X., Rioual, P., Qin, X., Liu, Z., Xiong, H., Yu, J., 2011. Hydrogeochemistry of three watersheds (the Erlqis, Zhungarer and Yili) in northern Xinjiang, NW China. Appl. Geochem. 26, 1535–1548.
Zwick, W.R., Velicer, W.F., 1986. Comparison of five rules for determining the number of components to retain. Psychol. Bull. 99, 432–442.